# Google Earth Engine and Artificial Intelligence for Earth Observation

## Algorithms and Sustainable Applications

**Edited by**

Vishakha Sood, Dileep Kumar Gupta, Sartajvir Singh, Biswajeet Pradhan

ELSEVIER

Earth Observation Series

Chapter 21

# Application of analytic hierarchy process for mapping flood vulnerability in Odisha using Google Earth Engine

**Pulakesh Pradhan, Ranjana Bajpai and Sribas Patra**
*Department of Geography, Ravenshaw University, Cuttack, Odisha, India*

## 1. Introduction

Floods are a prevalent natural disaster leading damage to life, property, infrastructure, natural settings, and economy almost every year (Sam et al., 2017). In recent times, the frequency of extreme weather events and its intensity has increased significantly (Beura, 2018; Arora et al., 2019; Mishra and Satapathy, 2020; NRSC, 2023). Floods are a recurring natural disaster that frequently occurs in Southeast Asia. Asian countries are especially vulnerable for the flood associated mortalities (Qin et al., 2022). India ranks among the top 10 countries that experience frequent occurrences of flooding. It is the second highest in terms of fatalities caused by riverine flooding and the third highest in terms of the overall estimated damage caused by floods (Senan et al., 2023). Current global estimation for flood related loss is approximately $6 billion per year and projected to increase $52 billion by 2050 (Hsu et al., 2017). India is highly susceptible to flooding due to its expansive coastal plains and agrarian society. In recent times urban floods are also increasing, which is also a matter of concern (Pathan et al., 2022; Roy Chowdhury and Parida, 2023). Climate change influences through rising temperatures, extremely localized precipitations and sea-level rise further exacerbate the intensity and frequencies of such flooding events (Mirza, 2003; Hirabayashi et al., 2013).

Flood disasters pose a severe threat to Odisha state situated along India's east coast in the Bay of Bengal. Intersected by four major systems with substantial catchment areas, Odisha witnesses recurrent floods triggered by heavy monsoons, cyclonic storms and inadequate carrying capacities of

**Google Earth Engine and Artificial Intelligence for Earth Observation**
https://doi.org/10.1016/B978-0-443-27372-8.00025-8

channels (Beura, 2018; Padhan and Madheswaran, 2023). Socioeconomic factors such as high population density and limited availability of advanced disaster management capacities further aggravate the impacts of floods. Climate projections indicating a rise in extreme precipitation events over the 21st century, robust flood risk assessment frameworks are needed to strengthen Odisha's resilience (Padhan and Madheswaran, 2023). Recent advancements in geospatial technologies provide scope for large-scale, analytical assessment of differential vulnerabilities faced by districts and guiding targeted adaptation efforts (Swain et al., 2020). In such a condition urgent attention toward disaster risk reduction policies are very much required (Patel et al., 2019). The hydro-meteorological settings with four major basins, intense monsoons and frequent cyclones render Odisha greatly susceptible to floods (Mohapatra et al., 2021). Barely recovering from past devastations, extreme flood episodes in recent years severely debilitated the Mahanadi basin impacting over 0.8 million citizens (Beura, 2018; Surwase et al., 2019). Distress migration and malnutrition levels also escalated post floods (Bahinipati, 2014; Mishra et al., 2017).

Padhan and Madheswaran (2023) investigated intensifying socio-economic vulnerabilities facing rural households in Odisha using hydro-meteorological data and government damage estimates. Increasing landlessness, marginalization and poverty compelled distressed out-migration post floods. The early warning communication system and the employment guarantee schemes effectively minimized losses during disasters. In their study, Mishra et al. (2016); Patel et al. (2019) studied the 2008 floods in Odisha with the help of meteorological reports and primary household surveys and found that the flood affected almost 0.8 million people and its economic loss exceeded $450 million, with the agriculture sector being the most severely affected. Low lying Balasore, Cuttack, Jajpur, and Kendrapara reported maximal fatalities and housing destruction, demanding priority rehabilitation. Sam et al. (2017) analyzed links between vulnerability, disasters, and adaptation in 7 Asian Least Developed Countries (LDCs) including India using statistical regressions. Adaptive capacities strongly correlated with literacy rates and socio-economic status. Community involvement, decentralization, and gender-sensitive planning were indispensable for resilience building against rising climate risks. Lele et al. (2013) suggested that India's highly engineering-focused approach to floods requires balancing with ecological, social, and participatory strategies enhancing preparedness of vulnerable communities. Floodplain zoning implementation also remains limited, escalating exposure. Updating codes to integrate climate projections is vital. Swain et al. (2020) highlighted the value of data-driven approaches enabled by geospatial analytics in addressing data challenges for large scale vulnerability mapping across entire states such as Odisha. Flexible frameworks allow continuous assimilation of updated satellite archives, census inputs etc. for robust policy insights. The analytical hierarchy process represents a robust and structured multicriteria decision-making technique allowing incorporation of qualitative

and quantitative data within the same framework using expert judgments for systematic indicator weighting (Swain et al., 2020; Gupta and Dixit, 2022). By enabling pairwise comparison between various vulnerability parameters, AHP allows assigning relative weights and aggregating composite indices in a transparent, consistent, and reproducible manner (Rautela et al., 2023). This eliminates subjectivities associated with arbitrary weight assignments common for data scarce regions (Meshram et al., 2019; Swain et al., 2020; Khosravi et al., 2024). Easy accommodation of new indicators within the hierarchical structure also improves policy insights (Swain et al., 2020; Gupta and Dixit, 2022; Rautela et al., 2023). These strengths underpin the extensive applications of AHP worldwide for flood vulnerability evaluations associated with climate risks. With climate change projected to amplify extreme precipitation events and resultant flooding for regions such as India (Bahinipati, 2014; Padhan and Madheswaran, 2022; NRSC, 2023), AHP integrations within geospatial technologies and climate models foster actionable adaptation roadmaps for disaster management departments through identification of changing spatial risk contours. Mainstreaming AHP usage by allocating adequate technical capacities can thus help strengthen evidence-based planning for enhancing community resilience.

## 2. Study area

Odisha is a coastal state located on the eastern side of India, adjacent to the Bay of Bengal. It is bounded by West Bengal and Jharkhand in northern part and Chhattisgarh and Andhra Pradesh in the western part of the state. It has a diverse landscape with mountains comprising its western region and plains spanning the central coastal belt. Four major rivers—Mahanadi, Brahmani, Baitarani and Subarnarekha flow across the state. Odisha has rich vegetation cover and receives abundant rainfall during the summer monsoon season (Figs. 21.1 and 21.2).

It has a tropical climate with very heavy monsoon rains averaging annual rainfall of 1400 mm, which is almost 95% of the yearly total (Mishra and Satapathy, 2020). During that time period major rivers named above flow through plains. Odisha frequently hit by cyclones between June and October, which also brings extreme rains. As per recent studies almost 30,000 sq. km out of 155,707 sq.km area prone to floods (Bahinipati, 2014; Mishra and Satapathy, 2020; Roy Chowdhury and Parida, 2023).

The 2008 floods submerged 20 districts after Cyclone Nisha dropped intense rainfall exceeding records (Kumari and Deo, 2020). Scientists predict further intensification of heavy rainfall events under climate change due to rising temperatures. Deforestation over decades has reduced drainage capacities while rapid and unplanned urbanization has replaced wetlands and farmlands with concrete surfaces. With over 39% of households engaged in small-scale, climate-sensitive agriculture on erosion-prone banks (Lele et al.,

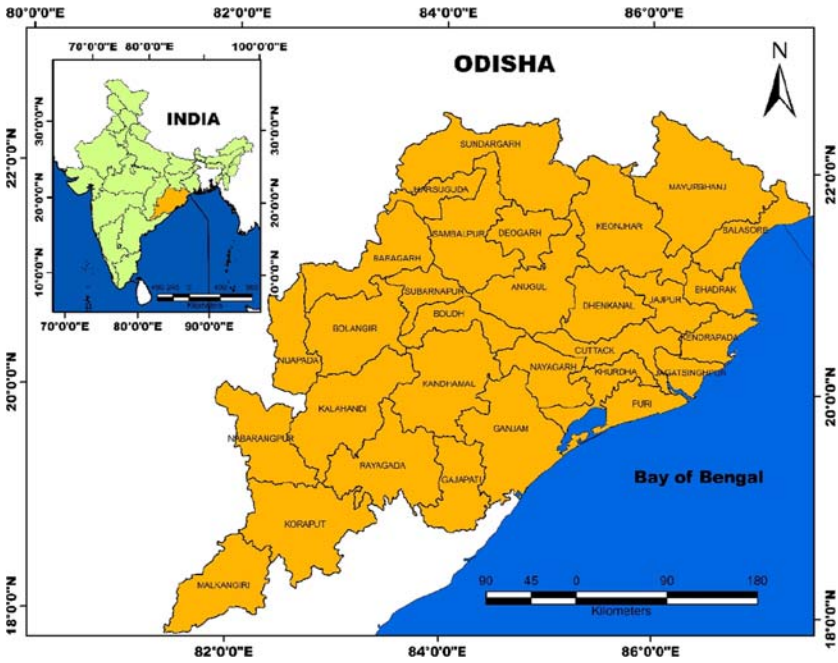


**FIGURE 21.1** Location map of Odisha.

2013), socioeconomic vulnerability persists. Embankments provide temporary protection but delayed rehabilitation leaves communities continually at risk. As per the Intergovernmental Panel on Climate Change (IPCC) models project increased summer and postmonsoon flooding for Asian basins (Hirabayashi et al., 2013). Though Odisha has already seen more frequent floods after an earlier decline (Mirza, 2003), sea level rise and tropical cyclone impacts pose novel adaptation challenges (Swain et al., 2022). Growing cities such as Bhubaneshwar and Cuttack have undergone extensive development and reducing floodwater absorption (Swain et al., 2023). Blocked drains and sewage lines frequently overflow, causing waterlogging (Danumah et al., 2016; Hsu et al., 2017). Urgent priority on vulnerability assessments, zoning policies, resilient infrastructure, and warning systems can build adaptive capacity (Wijesinghe et al., 2023).

## 3. Database

This study uses different types of data to study flood vulnerability in the state of Odisha. Details about each dataset given below to derived the major indicator for this study such as drainage, elevation, slope, land cover, soils, precipitation, and vegetation are given below (Table 21.1).

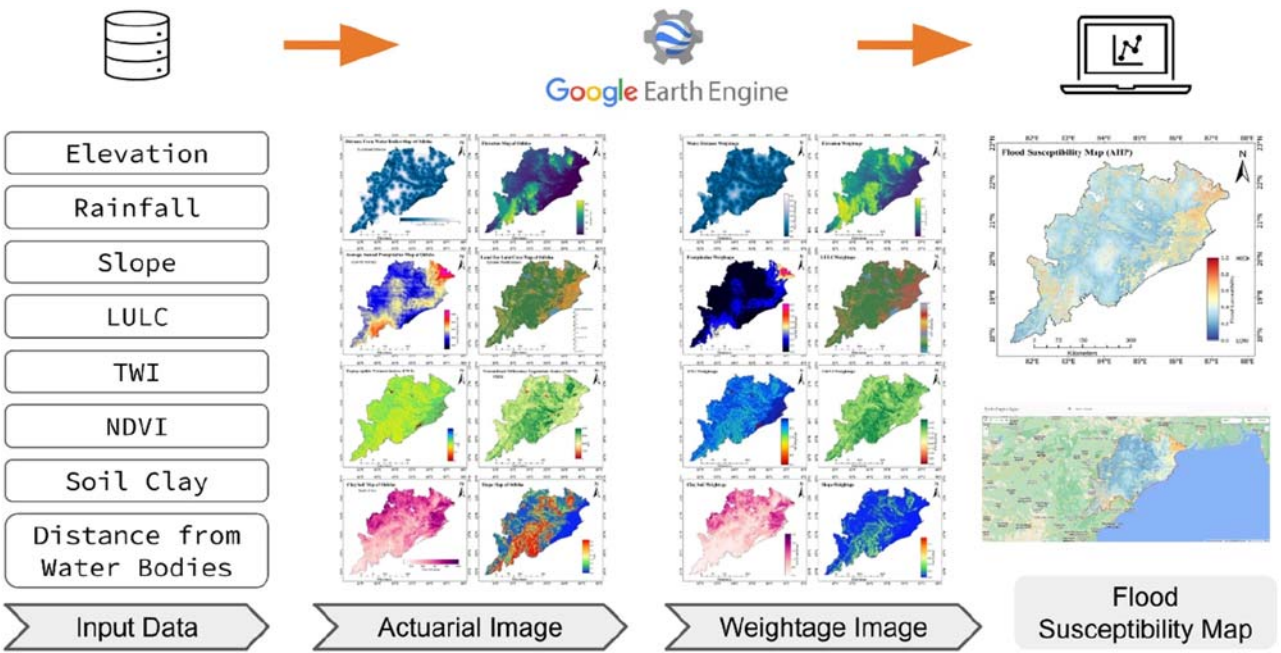


**FIGURE 21.2** Flow diagram of methodology.

**TABLE 21.1 Datasets used in the study.**

| Data type | Name | Sources | Resolution (mts.) |
|---|---|---|---|
| Spatial data | Distance from water bodies | GLCF: Landsat global inland water | 30 |
| | Elevation | NASA SRTM digital elevation | 30 |
| | Rainfall | CHIRPS Pentad (V2) | 5566 |
| | LULC | Google dynamic world (V1) | 10 |
| | TWI | WWF HydroSHEDS flow accumulation (15 arc Sec) | 463.83 |
| | NDVI | MOD13A1.061 | 500 |
| | Soil clay | ISRIC SoilGrids250m | 250 |
| | Slope | NASA SRTM digital elevation | 30 |

## 3.1 Hydrology (drainage and water bodies)

The HydroSHEDS network product provides vector hydrographic data mapped globally at 15 arc-second resolutions (approximately 500 m at the equator). It leverages elevation data from NASA's SRTM to derive consistent hydrological information including stream channels, watershed boundaries, flow directions, and flow accumulations. The free flowing layer maps the locations of nonobstructed, serving as the primary input to delineate floodplain extents based on adjoining topography. HydroSHEDS offers a standardized hydrographic mapping layer for large-scale hydrological analysis and flood risk modeling (Fig. 21.3A).

## 3.2 Elevation

The global digital elevation model with near-global coverage from NASA's Shuttle Radar Topography Mission (SRTM) has a resolution of 30 m and is used as the terrain basemap for extracting floodplain geomorphology. The refined SRTM Plus version applied corrects artifacts and voids in the original SRTM data using other global Digital Elevation Models (DEMs) from ASTER, GMTED, and NED. Precise elevation data enables basin delineation, flow accumulation modeling, and floodplain mapping based on adjoining topography. As the HydroSHEDS s are derived from SRTM, the two datasets exhibit strong vertical and horizontal positional accuracy. NASA SRTM topography underpins flood hazard characterization by delineating floodable terrain according to hydraulic modeling (Fig. 21.3B).

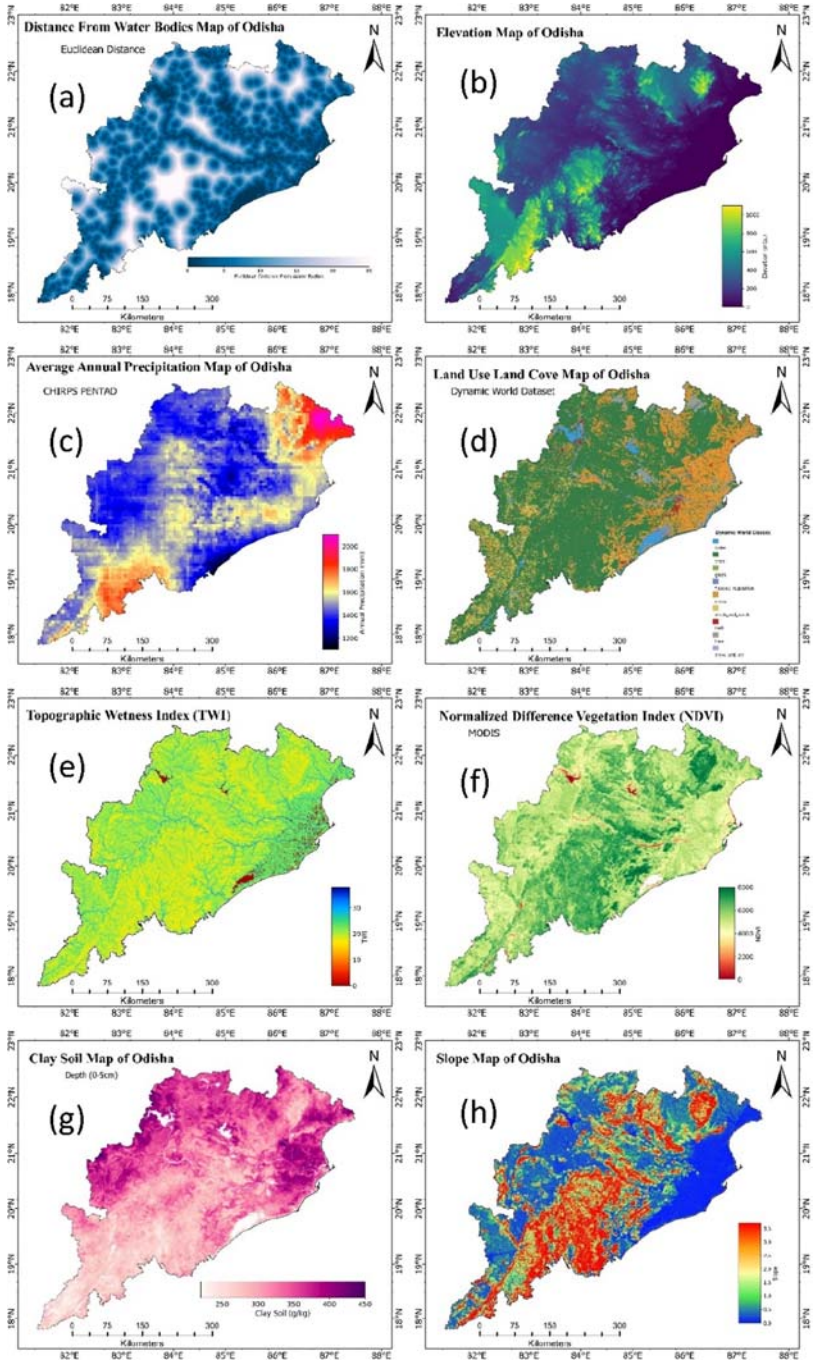


**FIGURE 21.3** (A) Distance from water bodies (B) elevation (C) precipitation (D) land use land cover (E) Topographic wetness index (F) NDVI (G) clay soil, (H) slope map of Odisha.

### 3.3 Slope

Derived numerically from SRTM level 2 data products, slope incorporates source positional and interferometric processing error estimates for enhanced precision confidence assessments. Slope supports variable flow routing modeling incorporating Darcy−Weisbach friction parameterizations. Adjusts flood wave velocity and erosion sensitivity (Fig. 21.3H).

### 3.4 Land cover (Google Dynamic World)

The Dynamic World dataset produced by Google provides recent 10 m global land cover classification derived from Sentinel-2 satellite imagery. Utilizing a deep neural network approach, Dynamic World delineates land cover distributions and subpixel class fractions since 2015 with frequent 2−5 day recurrence. Nine land cover categories are mapped ranging from forests, shrublands, and grasslands to croplands, wetlands, urban, barren, snow/ice, and open water. Characterizing the land cover types and distributions within floodplains constitutes a key model parameterization for surface roughness, infiltration rates, runoff potential, and damage exposure. Dynamic World land cover enables differentiating vulnerability by activity types occupying flood zones (Fig. 21.3D).

### 3.5 Soils (SoilGrids250m)

The global SoilGrids product from ISRIC (International Soil Reference and Information Center) provides critical soil property maps at 250 m resolution based on machine learning applied to over 150,000 soil profiles. Soil attributes modeled include clay fraction, organic carbon, bulk density, pH, and depth to bedrock among others. Soil characteristics directly influence the infiltration potential and runoff generation across landscapes, serving as key physical susceptibility factors for flooding. By distinguishing soil profiles floodplains, variable subsurface absorption capacities can be integrated within flood risk models to map differential vulnerabilities. SoilGrids fills a critical global data gap in characterizing subsurface floodplain properties (Fig. 21.3G).

### 3.6 Topographic Wetness Index

The TWI calculated from the HydroSHEDS Flow Accumulation (15 Arc-Seconds) datasets and SRTM DEM datasets with applying proper formula. It has a 463.83 m spatial resolution. It is a key input for the flood vulnerability analysis. By quantifying upstream area draining into each pixel, it identifies low-lying regions prone to flooding. Combined with factors such as slope, land use, and soil infiltration in a GIS analysis, HydroSHEDS allows ranking flood susceptibility across a study area. Its 15 arc-second resolution provides

sufficient detail for watershed analysis. As an objective hydrologic modeling input, HydroSHEDS integrates physical flooding factors into vulnerability assessment (Fig. 21.3E).

### 3.7 Precipitation (CHIRPS)

The Climate Hazards Group Infrared Precipitation with Stations (CHIRPS) dataset offers a comprehensive global rainfall record at a resolution of 5 km, spanning from 1981 to the present. CHIRPS incorporates satellite imagery with ground station precipitation data to create consistent rain gauge corrected time series for drought and flood trend analysis. Extreme precipitation patterns drive streaming and overland flood events, quantified by CHIRPS' 0.05° resolution satellite/station blended products. Subseasonal CHIRPS Pentad data enables identifying anomalously intense rainfall episodes over recent decades to help locate and characterize flooding responses across floodplains worldwide (Fig. 21.3C).

### 3.8 Vegetation (MODIS NDVI)

Moderate Resolution Imaging Spectroradiometer (MODIS) satellites operated by NASA provide regular global coverage up to daily timesteps since 1999 at resolutions ranging 250−1000 m. MODIS optical imagery is utilized to derive the NDVI, quantifying vegetation density and health based on measured near infrared and red spectral reflectance. As vegetation modulates terrain infiltration and flooding patterns, the MODIS NDVI layers help characterize floodplain land surface conditions and spatially variable runoff potential. NDVI facilitates differentiating vulnerabilities across vegetated floodplains, an important inundation parameter (Fig. 21.3F).

## 4. Methodology

The study employs the methodology of estimating the factors that contribute to floods in the specific area being investigated and assessing areas that are prone to flooding using the MCDM-AHP technique (Fig. 21.2).

### 4.1 Google Earth Engine

Google Earth Engine (GEE) provides a cloud-based platform offering advanced computational capabilities for processing huge geospatial and satellite data archives for environmental modeling, pattern detections and time-series analyses unconstrained by hardware limitations (Gorelick et al., 2017). The petabyte catalog allowing historical comparisons combined with JavaScript APIs for customized analyses foster rapid development of location intelligent solutions and real-time large-scale disaster management dashboards (Gorelick et al., 2017). These unique advantages offered by Google Earth Engine coupled with its free access have spurred its usage across recent flood

studies seeking improved granularity and operational outputs aligned with current ground scenarios for strengthening local resilience.

Although GEE is a powerful tool for geospatial analysis, it requires JavaScript or Python coding skills (Gorelick et al., 2017). This means that nonprogrammers may find it difficult to use. GEE has quota limits for the number of requests and exports, making it difficult for large-scale analysis (https://developers.google.com/earth-engine/guides/usage). It has limited customization beyond the provided tools and APIs. Cloud connectivity raise potential privacy concerns for sensitive data. Apart from that it requires good internet connectivity for efficient working.

## 4.2 Analytical hierarchy process

The Analytical Hierarchy Process (AHP) developed by Saaty (1987) constitutes an extensively applied multicriteria decision-making technique for complex prioritization and evaluation problems across areas such as sustainability planning, risk mappings, resource optimization, etc (Dahri and Abida, 2017; Mekonnen et al., 2023). By enabling systematic deconstruction of decision problems into a set of hierarchical indicators, AHP allows meaningful relative comparisons between parameters using simple pairwise comparison matrices (Tempa, 2022). This gives a robust and transparent means of generating criteria weights, tackling inconsistencies, and accommodating both qualitative and quantitative indicators within the same framework (Wijesinghe et al., 2023) (Table 21.2).

**TABLE 21.2 Magnitude for pare-wise comparison.**

| Numerical rating | Preferences |
|---|---|
| 1 | Equally preferred |
| 2 | Equally to moderately |
| 3 | Moderately preferred |
| 4 | Moderately to strongly |
| 5 | Strongly preferred |
| 6 | Strongly to very strongly |
| 7 | Very strongly preferred |
| 8 | Very strongly to extremely |
| 9 | Extremely preferred |

The ability of AHP techniques to intrinsically account for the often intangible, complex, and nuanced interlinkages shaping differential distributions of flood vulnerability across space makes it well suited for vulnerability science and climate adaptation research (Hsu et al., 2017; Sam et al., 2017). The participative determination of criteria significance also aids conflict resolution between multiple stakeholders while improving collective preparedness against escalating climate uncertainties (Nahin et al., 2023). From regional scale community-based studies to national level policy guidance, AHP constitutes a versatile tool. For instance, Sam et al. (2017) employed AHP-driven expert weighting of physical exposure, socio-economic fragility and resilience factors followed by GIS overlays to determine high flood risk in Odisha zonal level. Wijesinghe et al. (2023) adopted questionnaire surveys among multiple provincial stakeholders coupled with GIS infrastructure inventories for relative ranking of resilience indicators using AHP toward framing an overall Sri Lankan flood security strategy. Such research evidences the strengths of AHP to aid transparent and reproducible evaluation frameworks tackling complex risk problems across scales (Table 21.3).

### 4.3 Consistency check

The suggestion was made to validate the constructed pair-wise matrix and its weighting by assessing the Consistency Ratio (CR), which should have a value of 0.10 or lower (Saaty, 1987) (Eq. 21.2). Using the calculated Eigenvector matrix, a Consistency Index of 0.083 was determined, indicating a satisfactory set of decisions.

$$CR = \frac{CI}{RI}$$

Where $RI$ is the random index, and $CI$ is the consistency index.

$$CI = \frac{\lambda_{\max} - n}{n - 1}$$

where $\lambda_{max}$ is the largest or principal eigenvalue of the matrix that has calculated from the matrix, and $n$ is the order of the matrix (Tables 21.4–21.7).

### 4.4 Function used to assign weightage for each class in Google Earth Engine

```
function assignWeightage(image, minValue1, midValue2, midValue3, midValue4, weightage1, weightage2,
weightage3, weightage4, weightage5) {
  return (image.where(image.lt(minValue1), image.multiply(weightage1))
          .where(image.gte(minValue1).and(image.lt(midValue2)), image.multiply(weightage2))
          .where(image.gte(midValue2).and(image.lt(midValue3)), image.multiply(weightage3))
          .where(image.gte(midValue3).and(image.lt(midValue4)), image.multiply(weightage4))
          .where(image.gte(midValue4), image.multiply(weightage5)));
}
```

**TABLE 21.3** $8 \times 8$ Pair-wise comparison decision matrix.

| Factors | Water distance | Elevation | Rainfall | LULC | TWI | NDVI | Soil clay | Slope |
|---|---|---|---|---|---|---|---|---|
| Water distance | 1 | 3 | 4 | 3 | 5 | 7 | 5 | 8 |
| Elevation | 1/3 | 1 | 3 | 2 | 4 | 5 | 4 | 6 |
| Rainfall | 1/4 | 1/3 | 1 | 1/2 | 2 | 3 | 2 | 5 |
| LULC | 1/3 | 1/2 | 2 | 1 | 2 | 4 | 2 | 5 |
| TWI | 1/5 | 1/4 | 1/2 | 1/2 | 1 | 3 | 1 | 4 |
| NDVI | 1/7 | 1/5 | 1/3 | 1/4 | 1/3 | 1 | 1/3 | 2 |
| Soil clay | 1/5 | 1/4 | 1/2 | 1/2 | 1 | 3 | 1 | 4 |
| Slope | 1/8 | 1/6 | 1/5 | 1/5 | 1/4 | 1/2 | 1/4 | 1 |
| **Total** | **2.58** | **5.70** | **11.53** | **7.95** | **15.58** | **26.50** | **15.58** | **35.00** |

**TABLE 21.4** Normalized pair-wise comparison and weight values.

| | Water distance | Elevation | Rainfall | LULC | TWI | NDVI | Soil clay | Slope | Sum | Sum/7 | % |
|---|---|---|---|---|---|---|---|---|---|---|---|
| Water distance | 0.39 | 0.53 | 0.35 | 0.38 | 0.32 | 0.26 | 0.32 | 0.23 | 2.77 | 0.35 | 34.65 |
| Elevation | 0.13 | 0.18 | 0.26 | 0.25 | 0.26 | 0.19 | 0.26 | 0.17 | 1.69 | 0.21 | 21.12 |
| Rainfall | 0.10 | 0.06 | 0.09 | 0.06 | 0.13 | 0.11 | 0.13 | 0.14 | 0.82 | 0.10 | 10.22 |
| LULC | 0.13 | 0.09 | 0.17 | 0.13 | 0.13 | 0.15 | 0.13 | 0.14 | 1.07 | 0.13 | 13.33 |
| TWI | 0.08 | 0.04 | 0.04 | 0.06 | 0.06 | 0.11 | 0.06 | 0.11 | 0.58 | 0.07 | 7.29 |
| NDVI | 0.06 | 0.04 | 0.03 | 0.03 | 0.02 | 0.04 | 0.02 | 0.06 | 0.29 | 0.04 | 3.60 |
| Soil clay | 0.08 | 0.04 | 0.04 | 0.06 | 0.06 | 0.11 | 0.06 | 0.11 | 0.58 | 0.07 | 7.29 |
| Slope | 0.05 | 0.03 | 0.02 | 0.03 | 0.02 | 0.02 | 0.02 | 0.03 | 0.20 | 0.02 | 2.50 |
| | **1.00** | **1.00** | **1.00** | **1.00** | **1.00** | **1.00** | **1.00** | **1.00** | **8.00** | **1.00** | **100.00** |

| TABLE 21.5 Principal Eigen value. | | |
|---|---|---|
| **Water distance** | **0.35** | **0.90** |
| **Elevation** | 0.21 | 1.20 |
| **Rainfall** | 0.10 | 1.18 |
| **LULC** | 0.13 | 1.06 |
| **TWI** | 0.07 | 1.14 |
| **NDVI** | 0.04 | 0.96 |
| **Soil clay** | 0.07 | 1.14 |
| **Slope** | 0.02 | 0.87 |
| **PEV** | | **8.44** |

| TABLE 21.6 Consistency ratio (CR) and consistency index (CI). | |
|---|---|
| **CI** | 0.06268 (%) |
| **CR** | **4.446** |

## 5. Results

The present study utilizes the Multicriteria Decision-Making - Analytical Hierarchy Process (MCDM-AHP) model to prepare flood vulnerability zones (FVZ) mapping for the Odisha districts located in eastern part of India. Odisha is one of the major flood-prone states of the country, almost every year affected by devastating floods during the monsoon season due to extreme rainfall events and cyclones.

Eight influencing factors – Water Distance, Elevation, Rainfall, LULC, TWI, NDVI, Clay Soil and Slope were used to form an $8 \times 8$ decision matrix. The consistency ratio (CR) was calculated as 0.0627, indicating acceptable consistency in the assigned weights to these parameters. In the MCDM-AHP analysis, water distance or distance form and all water bodies was assigned the highest weight at 0.346 followed by elevation (0.211), LULC (0.133), rainfall (0.102), soil (0.064) and elevation (0.055) (Fig. 21.4). The weighted overlay method was then utilized to overlay these layers and prepare the final flood vulnerability zonation map (Fig. 21.5).

**TABLE 21.7 Assigning weight for each criterion.**

| Sl. No. | Parameter | Normalized (0–1) | Vulnerability | Weightage in percentage (%) |
|---|---|---|---|---|
| 1 | Water distance | <0.2 | Very high | 35 |
| | | 0.2–0.4 | High | 30 |
| | | 0.4–0.6 | Medium | 20 |
| | | 0.6–0.8 | Low | 10 |
| | | 0.8< | Very low | 5 |
| 2 | Elevation | <0.2 | Very high | 35 |
| | | 0.2–0.4 | High | 30 |
| | | 0.4–0.6 | Medium | 20 |
| | | 0.6–0.8 | Low | 10 |
| | | 0.8< | Very low | 5 |
| 3 | Rainfall | <0.2 | Low | 5 |
| | | 0.2–0.4 | Low | 5 |
| | | 0.4–0.6 | Medium | 20 |
| | | 0.6–0.8 | High | 30 |
| | | 0.8< | Very high | 40 |
| 4 | TWI | <0.2 | Very low | 5 |
| | | 0.2–0.4 | Low | 10 |
| | | 0.4–0.6 | Medium | 20 |
| | | 0.6–0.8 | High | 30 |
| | | 0.8< | Very high | 35 |
| 5 | NDVI | <0.2 | Very high | 35 |
| | | 0.2–0.4 | High | 25 |
| | | 0.4–0.6 | Medium | 15 |
| | | 0.6–0.8 | Low | 15 |
| | | 0.8< | Very low | 10 |
| 6 | Soil clay | <0.2 | Very low | 5 |
| | | 0.2–0.4 | Low | 10 |
| | | 0.4–0.6 | Medium | 20 |
| | | 0.6–0.8 | High | 30 |
| | | 0.8< | Very high | 35 |

*Continued*

**TABLE 21.7 Assigning weight for each criterion.—cont'd**

| Sl. No. | Parameter | Normalized (0–1) | Vulnerability | Weightage in percentage (%) |
|---|---|---|---|---|
| 7 | Slope | <0.2 | Very high | 40 |
| | | 0.2–0.4 | High | 30 |
| | | 0.4–0.6 | Medium | 20 |
| | | 0.6–0.8 | Low | 5 |
| | | 0.8< | Low | 5 |
| 8 | LULC (Google Dynamic World) | Water | Very high | 20 |
| | | Trees | Medium | 10 |
| | | Grass | Low | 5 |
| | | Flooded vegetation | Very high | 25 |
| | | Crops | High | 15 |
| | | Shrub and scrub | Medium | 10 |
| | | Built | Medium | 10 |
| | | Bare | Low | 5 |
| | | Snow and ice | Very low | 0 |

## 5.1 Assessment of flood vulnerability zones (FVZ)

## 5.2 Spatial pattern of flood vulnerability in Odisha

Fig. 21.5 shows the spatial vulnerability of flood in Odisha. The intensity of Flood Vulnerability mainly categorized into five classes such as Very low, Low, Medium, High, and Very high. In Odisha Ganjam and Puri districts basically associated with highly vulnerable zone. This study noted that it is about 172.87 sq.km and 168.12 sq.km area that consist of very high vulnerable zone in Ganjam and Puri district respectively. It is seen most of the coastal parts of these two districts (Fig. 21.5). Balasore and Mayurbhanj districts lie in high vulnerability zone; it is also seen in Fig. 21.5. Bhadrak, Jajpur, Koraput, Sundargarh, Cuttack, and Bargarh districts consist of medium vulnerable zone. It is also found that Bolangir, Kalahandi, and Dhenkanal basically consist with the very low flood vulnerable zone in Odisha.

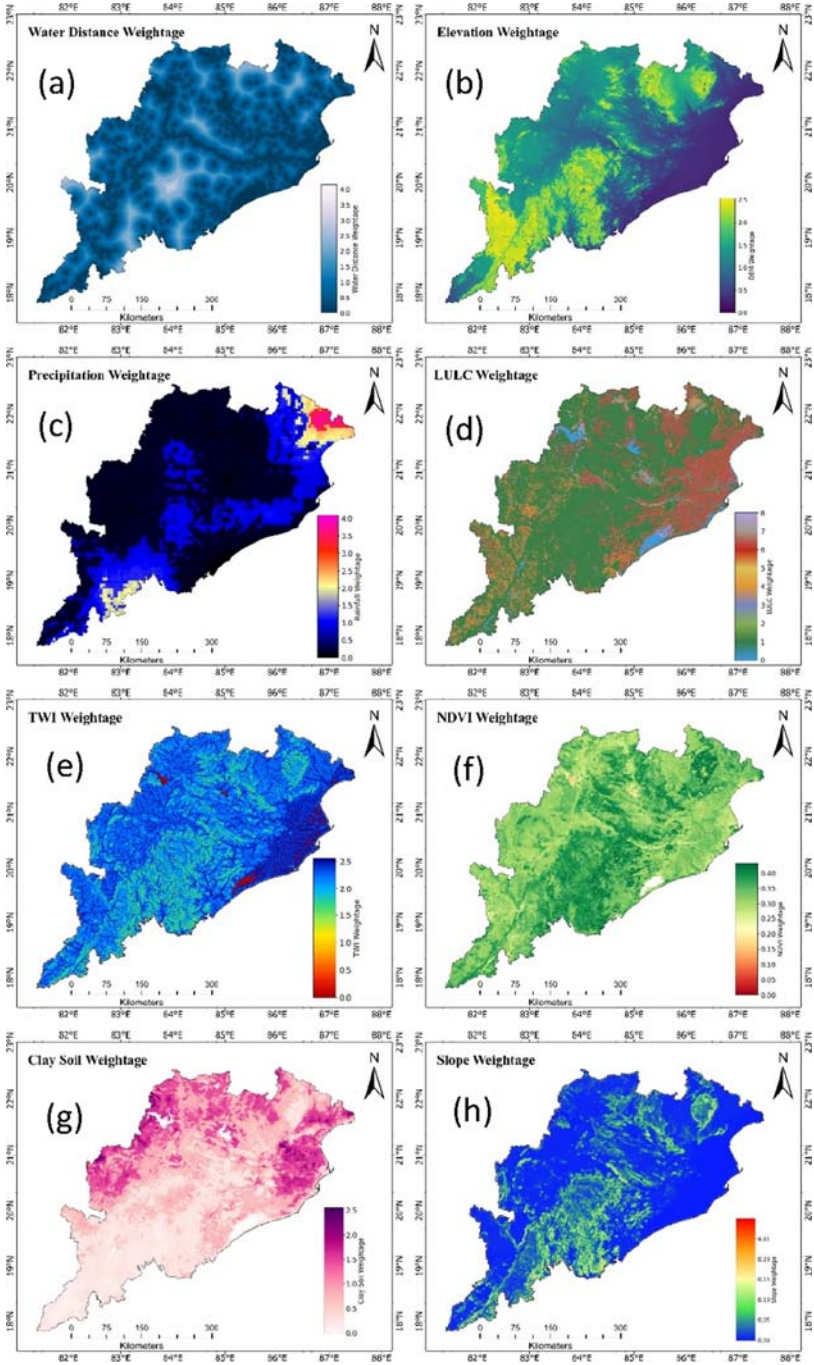


**FIGURE 21.4** Weightage assigned maps. (A) Distance from water bodies (B) elevation (C) precipitation (D) land use land cover (E) Topographic wetness index (f) NDVI (G) clay soil, (H) slope map of Odisha.

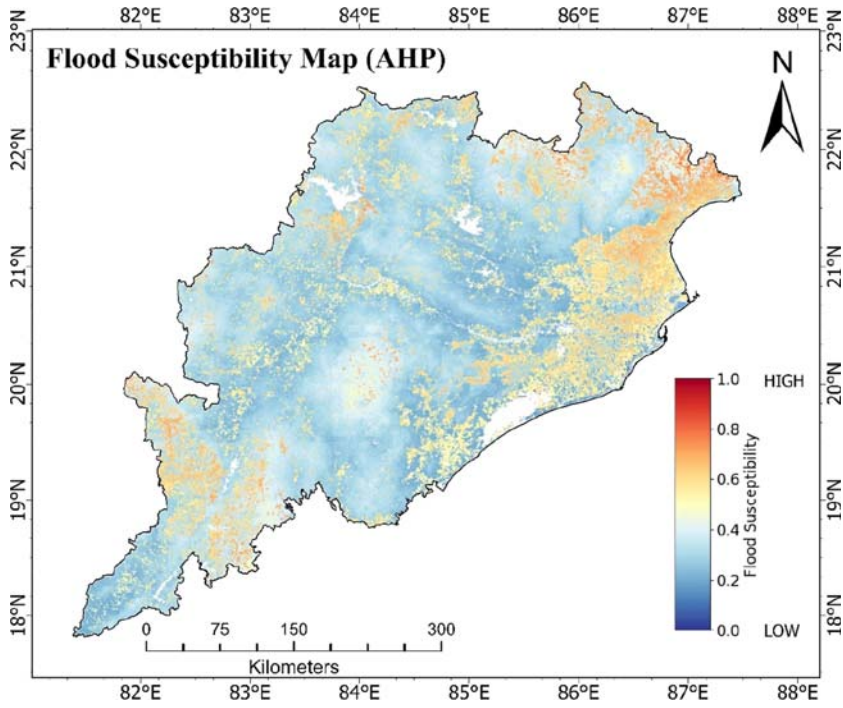


**FIGURE 21.5** Normalized flood susceptibility AHP map of state of Odisha.

The lack of resources and limited disaster management capacity to organize large-scale temporary relocations constrains the adaptation capability of most rural mountain communities in the region. Significant investments need to be made toward strengthening early warning systems for improved lead times, building additional shelter infrastructure at district and block levels, and providing technical and financial support to households for flood proofing of houses. Transparent designation of land parcels for relocation of vulnerable villages/settlements is also essential to reducing loss of lives and assets during disasters.

## 6. Discussion

Assessment of current and future vulnerabilities through modeling exercises as demonstrated in this study provides significant insights that can feed into evidence-based policy making for holistic and proactive flood risk management. Some of the key discussion points emerging from this analysis are.

### 6.1 Validation of models using historical data

The current vulnerability zoning model utilizes only a limited number of parameters based on data availability and analytical complexity

considerations. For higher accuracy, validation of model outputs is required using time series data of past flood events in Odisha in terms of number of houses damaged, agricultural areas inundated, population affected and loss of lives. This can help refine the influence of different vulnerability indicators.

### 6.2 Need for per pixel image classification

The traditional methods are based on mostly zonation. Biggest advantage of application of google earth engine in this case is per pixel vulnerability analysis. By doing this the small areas vulnerabilities can be identified. It will be very much helpful for accurate planning.

### 6.3 Dynamic modeling with Google Earth Engine

Factors such as rainfall, land use and vegetation cover are crucial in vulnerability analysis. These datasets are available in a regular interval basis in Google Earth Engine. With few lines of code changing, we can easily identify time defined vulnerability. As the dataset are dynamic, it will be giving results by the time frame user decided. The applicability of such dynamic map gives huge advantage for the respective authorities.

### 6.4 Socio-economic factors driving vulnerabilities

Beyond the natural system dynamics, socio-economic parameters such as population density, economic condition, house condition, social connectivity and also the climate variables also critically impact flood risk management. Future modeling efforts should aim to integrate pertinent census statistics and economic development plans to better understand changing vulnerabilities.

### 6.5 Linking with disaster management planning

The technical vulnerability modeling provides only one part of the information requirements for practical disaster management by local administration. These zones need to be overlaid with household level socio-economic data, shelter infrastructure maps, and inventory of search/rescue equipment and stockpile locations for emergency supplies. Only then comprehensive and executable flood response plans can be formulated with clear standard operating procedures defined for each identified risk zone.

## 7. Conclusion

The present study demonstrates a simple but effective approach utilizing widely available terrain, land use, soil, and climatic data to prepare detailed flood vulnerability zone mapping for a hazard prone the state of Odisha. Five

zones ranging from very low to very high were delineated based on multi-criteria analysis using key parameters such as slope, extreme rainfall intensity, etc. The study shows that apart from the natural landscape factors, increasing anthropogenic pressures from unplanned urbanization and tourism expansion are significantly enhancing the flood risks.

The analysis suggests a high preference for coping mechanisms relying on temporary relocation to safer areas or public shelters during flood events due to lack of resources for major structural protection measures. For strengthening community level adaptation in the region, specific recommendations include improving early warning systems, designating land for relocation of vulnerable settlements, enhancing shelter infrastructure, flood proofing of houses, and providing financial and technical support for nature-based solutions.

While the current model provides an initial assessment of flood prone areas, future research should focus on validating results using past flood damage data, integrating climate change projections and reservoir storage effects, and linking with district level disaster management plans. Overall, vulnerability zone mapping provides a quantitative, evidence-based support platform to guide adaptation investments, disaster contingency planning, and climate resilient development planning in such hazard prone regions.

## Appendix

1. **Google Earth Engine Code Link:** https://code.earthengine.google.com/c9dc3a15cd005f1f4f4b3fa400be0254
2. **Google Earth Engine APP link:** https://pulakeshpradhan.users.earthengine.app/view/ahpflood
3. **All Calculation Tables:** https://docs.google.com/spreadsheets/d/1IUUCP46KEQ9A2h0Ck9Xd-vlyS4fbqhng/edit?usp=sharing&ouid=107092937379500639027&rtpof=true&sd=true

## Acknowledgments

The authors would like to thank the Google Earth Engine for providing data and advanced computing for free of cost.

## Funding

NA.

## References

Arora, A., Bansal, S., Ward, P.S., 2019. Do farmers value rice varieties tolerant to droughts and floods? Evidence from a discrete choice experiment in Odisha, India. Water Res. Econ. 25. https://doi.org/10.1016/j.wre.2018.03.001.

Bahinipati, C.S., 2014. Assessment of vulnerability to cyclones and floods in Odisha, India: a district-level analysis. Curr. Sci. 107 (12), 1997–2007.

Beura, D., 2018. Floods in Mahanadi river, Odisha, India. Int. J. Eng. Appl. Sci. 2 (2).

Dahri, N., Abida, H., 2017. Monte Carlo simulation-aided analytical hierarchy process (AHP) for flood susceptibility mapping in Gabes Basin (southeastern Tunisia). Environ. Earth Sci. 76 (7), 1–14. https://doi.org/10.1007/s12665-017-6619-4.

Danumah, J.H., et al., 2016. Flood risk assessment and mapping in Abidjan district using multi-criteria analysis (AHP) model and geoinformation techniques, (Cote d'Ivoire). Geoenviron. Dis. 3 (1). https://doi.org/10.1186/s40677-016-0044-y.

Gorelick, N., et al., 2017. Google earth engine: planetary-scale geospatial analysis for everyone. Rem. Sens. Environ. 202, 18–27. https://doi.org/10.1016/J.RSE.2017.06.031.

Gupta, L., Dixit, J., 2022. A GIS-based flood risk mapping of Assam, India, using the MCDA-AHP approach at the regional and administrative level. Geocarto Int. 37 (26). https://doi.org/10.1080/10106049.2022.2060329.

Hirabayashi, Y., et al., 2013. Global flood risk under climate change. Nat. Clim. Change 3 (9), 816–821. https://doi.org/10.1038/nclimate1911.

Hsu, T.W., et al., 2017. A study on coastal flooding and risk assessment under climate change in the mid-western coast of Taiwan. Water 9 (6), 1–13. https://doi.org/10.3390/w9060390.

Khosravi, Y., Homayouni, S., St-Hilaire, A., 2024. An integrated dryness index based on geographically weighted regression and satellite earth observations. Sci. Total Environ. 911, 168807. https://doi.org/10.1016/J.SCITOTENV.2023.168807.

Kumari, K., Deo, A.A., 2020. Effect of Indian ocean cyclone on coastal region using remote sensing and GIS. Int. J. Big Data Min. Glob. Warm. 02 (02). https://doi.org/10.1142/s2630534820500059.

Lele, S., et al., 2013. Environment and Development.

Mekonnen, T.M., Mitiku, A.B., Woldemichael, A.T., 2023. Flood hazard zoning of upper awash river basin, Ethiopia, using the analytical hierarchy process (AHP) as compared to sensitivity analysis. Sci. World J. 2023. https://doi.org/10.1155/2023/1675634.

Meshram, S.G., et al., 2019. Comparison of AHP and fuzzy AHP models for prioritization of watersheds. Soft Comput. 23 (24), 13615–13625. https://doi.org/10.1007/s00500-019-03900-z.

Mirza, M.M.Q., 2003. Three recent extreme floods in Bangladesh: a hydro-meteorological analysis. Nat. Hazards 28 (1), 35–64. https://doi.org/10.1023/A:1021169731325/METRICS.

Mishra, G.R., Das, B.C., Swain, P., Sardar, K., 2017. Awareness and preparedness level of livestock farmers during flood in Odisha, India. Int. J. Agric. Sci. Res. 7 (1).

Mishra, D., Satapathy, S., 2020. MCDM approach for mitigation of flooding risks in Odisha (India) based on information retrieval. Int. J. Cognit. Inf. Nat. Intell. 14 (2), 77–91. https://doi.org/10.4018/IJCINI.2020040105.

Mishra, D., Sahu, N.C., Sahoo, D., 2016. Impact of climate change on agricultural production of Odisha (India): a Ricardian analysis. Reg. Environ. Change 16 (2), 575–584. https://doi.org/10.1007/s10113-015-0774-5.

Mohapatra, S., Harish, V.S.K.V., Dwivedi, G., 2021. Climate change, cyclone and rural communities: understanding people's perceptions and adaptations in rural eastern India. Mater. Today: Proc. 49, 412–417. https://doi.org/10.1016/j.matpr.2021.02.384.

Nahin, K.T.K., et al., 2023. Flood vulnerability assessment in the Jamuna river floodplain using multi-criteria decision analysis: a case study in Jamalpur district, Bangladesh. Heliyon 9 (3), e14520. https://doi.org/10.1016/j.heliyon.2023.e14520.

NRSC, 2023. Flood Affected Area Atlas of India - Satellite Based Study, p. 165. https://ndma.gov.in/sites/default/files/PDF/FHA/Flood_Affected_Area_Atlas_of_India.pdf.

Padhan, N., Madheswaran, S., 2022. Determinants of farm-level adaptation strategies to flood: insights from a farm household-level survey in coastal districts of Odisha. Water Pol. 24 (2). https://doi.org/10.2166/wp.2022.218.

Padhan, N., Madheswaran, S., 2023. An integrated assessment of vulnerability to floods in coastal Odisha: a district-level analysis. Nat. Hazards 115 (3). https://doi.org/10.1007/s11069-022-05641-z.

Patel, S.K., et al., 2019. A review on extreme weather events and livelihood in Odisha, India. Mausam 70 (3), 551−560. https://doi.org/10.54302/mausam.v70i3.258.

Pathan, A.I., et al., 2022. AHP and TOPSIS based flood risk assessment- a case study of the Navsari City, Gujarat, India. Environ. Monit. Assess. 194 (7). https://doi.org/10.1007/s10661-022-10111-x.

Qin, Y., et al., 2022. Challenges threatening agricultural sustainability in central Asia: status and prospect. Int. J. Environ. Res. Publ. Health 19 (10), 6200. https://doi.org/10.3390/ijerph19106200.

Rautela, K.S., et al., 2023. Flood vulnerability assessment across alaknanda river basin using GIS-based combined analysis of geomorphometric approach and MCDM-AHP. J. Geol. Soc. India 99 (11), 1604−1615. https://doi.org/10.1007/s12594-023-2512-9.

Roy Chowdhury, J., Parida, Y., 2023. Flood shocks and post-disaster recovery of households: an empirical analysis from rural Odisha, India. Int. J. Disaster Risk Reduc. 97 (October), 104070. https://doi.org/10.1016/j.ijdrr.2023.104070.

Saaty, R.W., 1987. The analytic hierarchy process-what it is and how it is used. Math. Modell. 9 (5), 161−176.

Sam, A.S., et al., 2017. Vulnerabilities to flood hazards among rural households in India. Nat. Hazards 88 (2), 1133−1153. https://doi.org/10.1007/s11069-017-2911-6.

Senan, C.P.C., et al., 2023. Flood vulnerability of a few areas in the foothills of the Western Ghats: a comparison of AHP and F-AHP models. Stoch. Environ. Res. Risk Assess. 37 (2), 527−556. https://doi.org/10.1007/s00477-022-02267-2.

Surwase, T., et al., 2019. Novel technique for developing flood hazard map by using AHP: a study on part of Mahanadi River in Odisha. SN Appl. Sci. 1 (10). https://doi.org/10.1007/s42452-019-1233-6.

Swain, K.C., Singha, C., Nayak, L., 2020. Flood susceptibility mapping through the GIS-AHP technique using the cloud. ISPRS Int. J. Geo-Inf. 9 (12). https://doi.org/10.3390/ijgi9120720.

Swain, A.K., Mohapatra, P., Mishra, J., 2022. Temporal variations of Ndvi with responses to climate change in Mayurbhanj district of Odisha from 2015-2020. J. Technol. Innov. 2 (1), 11−15. https://doi.org/10.26480/jtin.01.2022.11.15.

Swain, M., et al., 2023. Delay in timing and spatial reorganization of rainfall due to urbanization-analysis over India's smart city Bhubaneswar. Comput. Urban Sci. 3 (1). https://doi.org/10.1007/s43762-023-00081-2.

Tempa, K., 2022. District flood vulnerability assessment using analytic hierarchy process (AHP) with historical flood events in Bhutan. PLoS One 17 (6 June), 1−20. https://doi.org/10.1371/journal.pone.0270467.

Wijesinghe, W.M.D.C., et al., 2023. Integrated flood hazard vulnerability modeling of neluwa (Sri Lanka) using analytical hierarchy process and geospatial techniques. Water 15 (6). https://doi.org/10.3390/w15061212.